Preparation and Characterization of Thermally Evaporated Octa Substituted Zinc Phthalocyanine Thin Films

Vinu T. Vadakel*, C.S. Menon

School of Pure and Applied Physics, Mahatma Gandhi University,
Priyadarshini Hills P.O, Kottayam 686560 Kerala, India

Thin films of Zinc Octakis Octyloxy Phthalocyanine (ZnPcOC$_8$) are prepared at a base pressure of 10^{-5} Torr using Hind Hi-Vac-12A4 thermal evaporation plant. The films are deposited onto precleaned glass substrates kept at room temperature. Absorption spectra of the films are recorded using the Shimadzu 160A UV-Visible spectrophotometer. The effect of post deposition annealing on the optical constants are studied. The nature of optical transition is found to be direct type. The optical band gap energy of the annealed samples remains almost the same. The invariance of the optical band gap shows the thermal stability of the material for optical applications. The X-ray diffraction analysis of vacuum evaporated films reveals that the crystallinity increases with increase in annealing temperature. The variation of the surface morphology with annealing is also studied using Scanning Electron Micrograph (SEM).

Keywords: Zinc octakis octyloxy phthalocyanine, Band gap energy, Optical parameters, XRD, SEM.

PACS numbers: 81.15kk, 78.20 – e, 78.20 ci

1. INTRODUCTION

In recent years there has been growing interest in the field of organic semiconducting films due to their successful application in optical and electronic devices such as LED's, display devices, field effect transistors and sensor devices [1-4]. The phthalocyanines (pc's) are a class of organic semiconductors with conjugate (alternate single and double bond) structure [5]. The crystal structure of these materials resembles that of chlorophyll and hence their photoconductive and photovoltaic properties have attracted a great deal of attention [6-8]. Adsorption of oxidizing or reducing gases on the surface of pc films induces change in their electrical conductivity [9]. Very recently these compounds have been successfully tested for the detection of volatile organic compounds and sedative drugs by optical techniques also [10-11]. Due to their strong absorption in the UV and Visible region, pc and its metal complexes have been considered as electrophotographic materials, optical recording media and nonlinear optical materials [12].

Metal pc's usually exist in several crystalline polymorphs, including α and β structures. The β form is the most stable one at room temperature. If MPc's are evaporated onto substrates at room temperature the α form will normally be obtained. Moreover it was reported that α-form can be converted into β-form by successive sublimation [13-14].

In this work the optical and structural properties of zinc phthalocyanine substituted with eight alkoxy chains in the peripheral (2, 3, 9, 10, 16, 17, 23, 24) positions with molecular formula C$_{96}$H$_{144}$N$_8$O$_8$Zn are investigated. There are no results available concering determination and characterisation of optical constants and structural studies on ZnPcOC$_8$. We have used thermal evaporation technique for the preparation of the films. The fundamental and trap level energy gaps are estimated and discussed. In addition the optical constants are determined. X-ray diffractograms have been recorded and analysed to determine the crystallinity of the films. These materials have the advantage of being sufficiently stable that they can be prepared as thin films by thermal evaporation technique.

2. EXPERIMENTAL

ZnPcOC$_8$ powder (with 95 % purity) procured from Sigma-Aldrich Company (USA) is used as the source material for the preparation of thin films. The molecular structure of the material is given in Fig. 1 Thin films of thickness 143 nm are prepared by vacuum sublimation from a resistively heated molybdenum boat using a "Hind Hi-Vac 12 A4" coating system. Thin films are deposited onto thoroughly cleaned rectangular glass substrates of dimension 4 cm × 1.2 cm × 0.1 cm at room temperature at a base pressure of 10^{-5} Torr. The thickness of the films is measured by Tolansky's multiple beam interference technique [15]. Thin films prepared at room temperature are annealed in air and vacuum at different temperatures for one hour in a programmable temperature controllabe furnace. UV-Visible absorption spectra are recorded in the wavelength range 200-900 nm using a Shimadzu 160A UV-Visible spectrophotometer. The structural studies have been carried out by the X-ray diffraction method (Cu K$_\alpha$ radiation, = 1.5418 Å). Scanning electron micrographs of the samples are taken by JEOL JSM-6390 Scanning Electron Microscope.

3. RESULTS AND DISCUSSION

3.1 Optical studies

The UV-Visible-NIR absorption spectra of as deposited and some annealed ZnPcOC$_8$ thin films of thickness 143 nm are given in Fig. 2. The basic 18 π electron structure in metal free and metallo-phthalocyanine molecules has very rich molecular orbital and available energy levels. The populated highest occupied molecular orbital (HOMO) and singlet highest occupied molecular orbital (SHOMO) levels are a_{14} (π) and a_{24}

---

* vinutvadakel@gmail.com
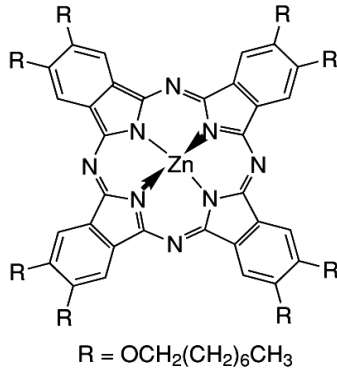
Fig. 1 – Molecular structure of ZnPcOC$_8$

Fig. 3 – Plot of α^2 vs $h\nu$ for as deposited sample

(π)and the first excited lowest unoccupied molecular orbitals (LUMO) level is e_g (π^*) The electronic transitions a_{14} (π) to e_g (π^*) are responsible for the intense visible absorption Q and ultraviolet Soret band (*B*) bands The Q absorption band splits arise as a result of vibrational conditions. [16]. All the absorption spectra consists of two main bands B and Q. The stability in the peak positions for the films annealed at different temperatures give an evidence of a stable structure of the films. The annealing process has an influence on the absorption coefficient of the investigated films. The positions of the peaks remain the same. The absorption edge is analysed using the theory of Bardeen et. al [17]. The absorbance α is related to bandgap energy E_g by the equation

$$\alpha h\nu = B(h\nu - E_g)^n \tag{1}$$

The trap levels are formed due to some types of defects present in the film. The formation of these defects is attributed to the unsaturated bonds. The formation of defects due to nitrogen, hydrogen, and oxygen ambient affect electrical conductivity, mobility and trap density. This in turn affect the position of the Fermi level [18] from Table 1. It is clear that the band gap and trap levels doesn't vary appreciably with annealing. Due to weak Van der Waal's interaction between the molecules in the film, their optical properties are not significantly changed when compared with free molecules.

Table 1 – Variation of band gap energy and trap level energy of ZnPcOC$_8$ thin films annealed at different temperatures

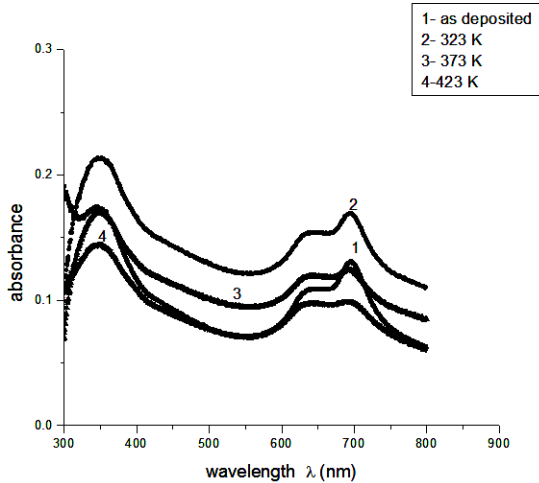| Sample	($E_g \pm 0.01$) eV	(Trap level ± 0.01) eV
as deposited	2.73	1.52
323K	2.70	1.54
373 K	2.72	1.53
423 K	2.75	1.50
473 K	2.74	1.49
523 K	2.73	1.48

Fig. 2 – Absorption spectrum of the ZnPcOC$_8$ thin films

where E_g is the bandgap energy, B – a constant nearly independent of photon energy and known as disorder parameter. Value of $n = 1/2$ for direct allowed transitions and $h\nu$ is the photon energy. A satisfactory fit is obtained for $n = 1/2$ and it indicates the exsistence of direct band gap. The band gap is determined by plotting $(\alpha h\nu)^2$ as a function of $h\nu$ and extrapolating the straight line region to the energy axis (Fig. 3). Such a plot for the as deposited sample is given in Fig. 3. The intercept at $(\alpha h\nu)^2 = 0$ gives the bandgap. The bandgap and sublevels as a function of annealing temperature are collected in Table 1.
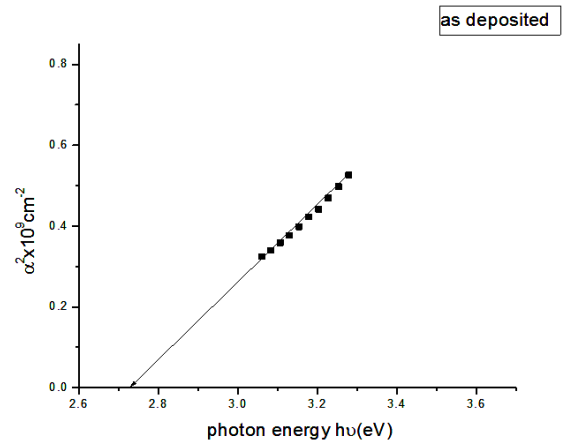
The fundamental optical parameters are determined from the transmittance and reflectance spectra of these thin films. The inequality $R + T < 1$ at shorter wavelength ($\lambda < 900$ nm) shows the existence of absorption . The reflectivity R of an absorbing medium of refractive index n and extinction coefficient k in air for normal incidence is given by

$$R = \frac{(n-1)^2 + k^2}{(n+1)^2 + k^2} \tag{2}$$

the extinction coefficient k is given by

$$k = \alpha\lambda/4\pi \tag{3}$$

Thus by knowing α and k, n is calculated. The optical properties of the films are characterized by the complex refractive index ($N = n - ik$) and the complex dielectric constant ($\varepsilon = \varepsilon_1 - i\varepsilon_2$). The real part ε_1 generally relates to dispersion, while the imaginary part ε_2 gives a measure of the dissipation rate of the wave in the medium [19].

The two parameters are related to n and k through the equation

$$\varepsilon_1 = n^2 - k^2 \qquad (4)$$

$$\varepsilon_2 = 2nk \qquad (5)$$

The values of k, n, ε_1, ε_2 are calculated using these equations. The dependence of photon energy on n and k ε_1 and ε_2 for the as deposited sample is plotted in Fig. 4 and 5 respectively.
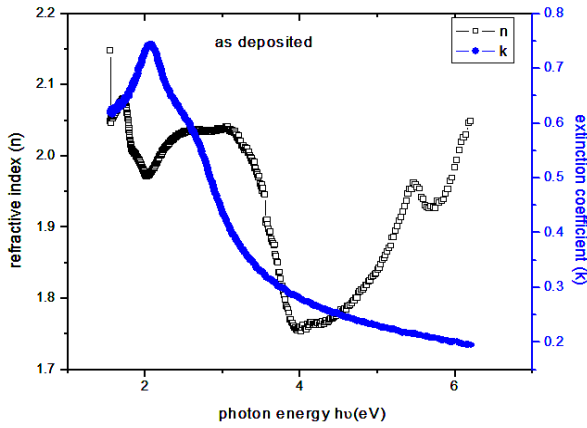

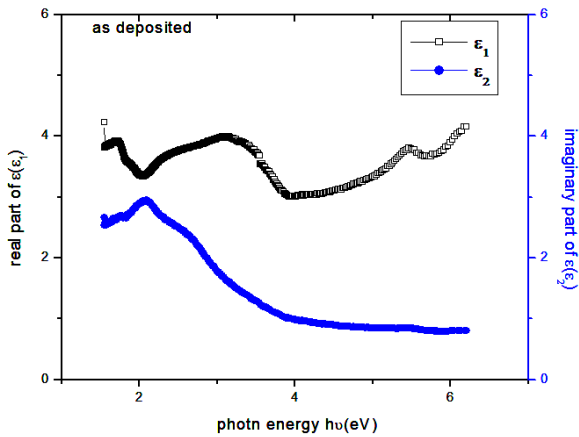**Fig 4** – Variation of n and k with photon energy for the as deposited film

Fig. 5 – Variation of ε_1 and ε_2 with photon energy for the as deposited film

The refractive index n has a maximum value of 2.08 at 1.69 eV. The extinction coefficient k has a maximum value of 0.75 at 2.04 eV. The real part ε_1 shows a maximum value of 1.70 at 3.92 eV while the imaginary part ε_2 has a maximum value of 2.92 at 2.07 eV.

3.2   EDAX analysis

An energy dispersive system was employed in the present studies in order to determine the various elements present in the films and their concentration. EDAX analysis confirms the composition of the constituents in the deposited films. Fig. 6 shows the EDAX spectrum of the as deposited film. From Fig. 6 the presence of Si and O peaks are due to glass substrates.

3.3   Structural Studies

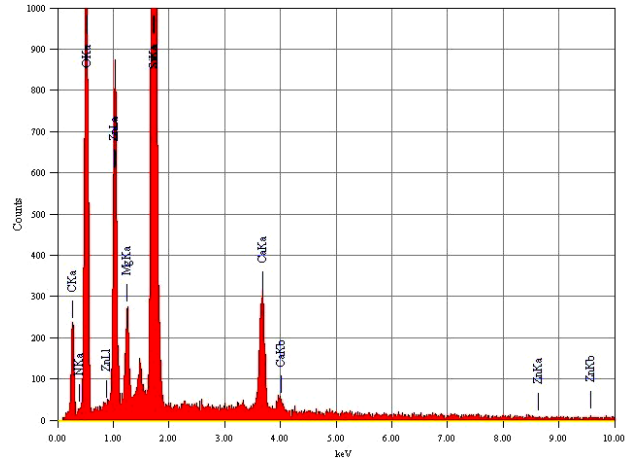The structural analysis for the bulk as well as the films were carried out by an X-ray diffractometer

Fig. 6 – EDAX spectrum of as deposited sample

(using CuK_α radiation with $\lambda = 1.5418$ Å). Fig. 7 shows the XRD pattern for the bulk $ZnPcOC_8$ powder and Fig. 8 that of the films annealed at different temperatures. The XRD pattern exhibits a crystalline nature. The crystallite size (D) is calculated using the Scherrer formula [20] from the full width at half maximum(FWHM) (β):

$$D = \frac{0.94\lambda}{\beta \cos\theta} \qquad (6)$$

The strain ε is calculated using the formula

$$\varepsilon = \beta \cos\theta / 4 \qquad (7)$$

The dislocation density δ is defined as the length of dislocation lines per unit volume of the crystal is evaluated from the formula
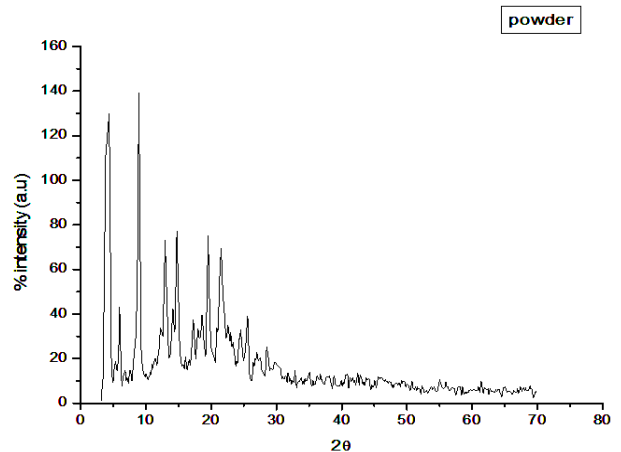

Fig. 7 – X-ray diffractiogram of bulk $ZnPcOC_8$ powder

$$\delta = \frac{1}{D^2} \qquad (8)$$

Table 2 shows the calculated values of crystallite size (D), strain (ε) and dislocation density (δ) for different annealing temperatures. Standard data's of $ZnPcOC_8$ powder is not available in literature. So indexing is not done. Table 3 shows the peak positions and d values of films annealed at different temperatures.
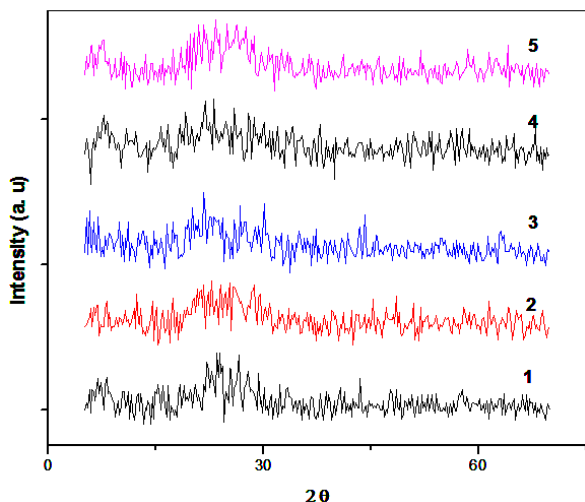
Fig. 8 – X-ray diffractograms of 1: as deposited, 2: annealed at 373 K, 3: annealed at 423 K, 4: annealed at 473 K, 5: annealed at 523 K

From the Fig. 8 it is observed that the crystallinity increases with increase in annealing temperature. The no. of peaks observed is more for the sample annealed at 373 K compared to as deposited film. But for the annealing temperature of 423 K the number of peaks is less. Further increase in temperature increases the number of peaks. The intensity of peaks is found to increase with the annealing temperature up to 473 K which is due to preferential orientation of more crystal planes. Microcrystallite grain size is found to increase in annealing temperature up to 473 K and for the sample annealed at 523 K, there is a decrease in grain size.

Table 2 – Comparative look of the crystallite size (*D*), strain (*ε*) and dislocation density (*δ*) for different annealing temperatures

| Sample	D (nm)	ε (10^{-4} lin^{-2} m^{-2})	δ (10^{15} lin m^{-2})
as deposited	20.83	1.74	2.30
373 K	14.08	2.57	5.04
423 K	21.11	1.72	2.24
473 K	21.19	1.71	2.27
523 K	16.13	2.24	3.84

Table 3 – Intense peak positions and *d* values of films annealed at different temperatures

Samples	2θ	d
As deposited	23.898	3.723
	26.419	3.373
373 K	21.313	4.168
	28.492	3.132
423 K	19.766	4.491
	34.891	2.557
473 K	21.826	4.072
	24.690	3.605
523 K	18.434	4.812
	11.780	3.782

3.4 Surface Morphology

The SEM images of ZnPcOC$_8$ films prepared at various annealing temperatures are shown in Fig. 9. As the annealing temperature increases, the film morphology changes. At room temperature small flower like structures with large flakes are observed. For the annealing temperature of 373 K clusters are observed. When the temperature increases the pattern changed. On increasing the annealing temperature some sort of cluster formation and small granules like structures are observed on the film surface.

a

b

c

d
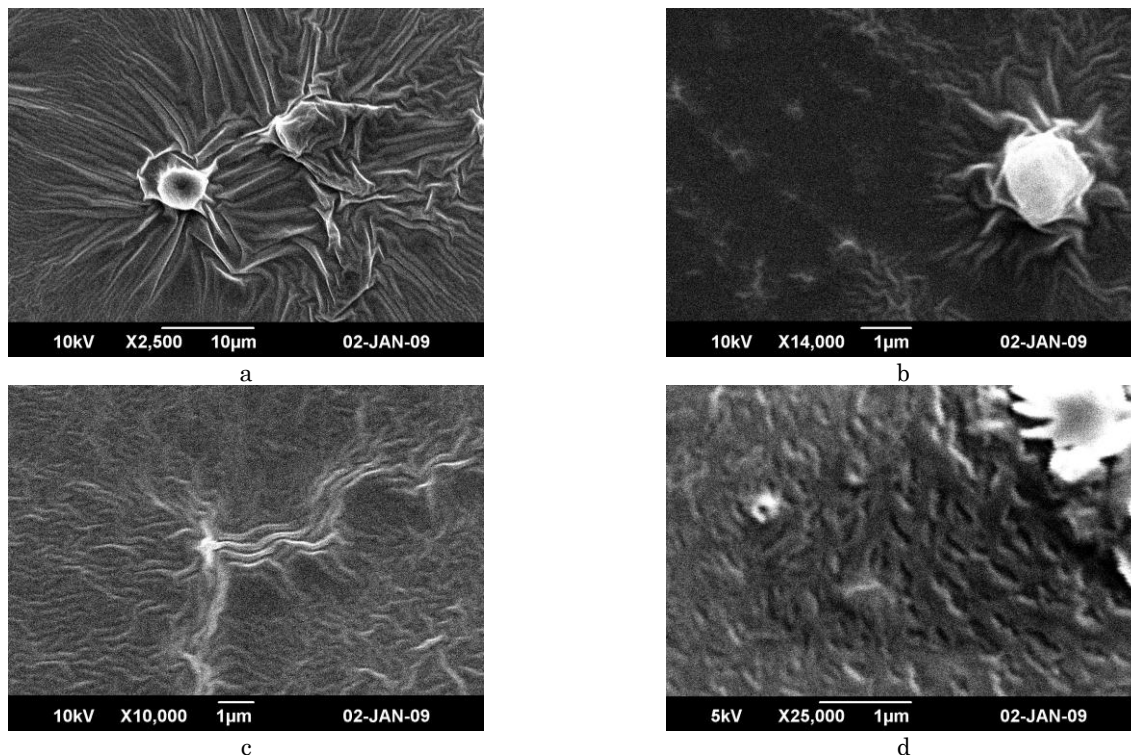
Fig. 9 – SEM images of A: as deposited B: annealed at 323 K, C: annealed at 373 K, D: annealed at 523 K

4. CONCLUSION

ZnPcOC$_8$ thin films are prepared by vacuum sublimation of ZnPcOC$_8$ powder and the fundamental properties are investigated. Since these thin films exhibit good absorption in the visible region of the electromagnetic spectrum, it can be a suitable candidate for photovoltaic applications. The optical transition in thin film is found to be direct and allowed. The band gap and trap levels shows no appreciable variation with annealing temperature. From the X-ray diffractograms, it is observed that as annealing temperature increases, the crystallinity of the films increases. The grain size is found to vary with the annealing temperature. By optimizing these parameters, these thin films can be used to fabricate organic semiconductor devices. SEM images for the as deposited film shows nano flower like structures while annealed samples show cluster formation.

REFERENCES

1. J.R. Ostrick, A. Dodabalapur, L. Torsi, A.J. Lovinger, E.W. Kwock, T.M. Miller, M. Galvin, M. Berggren, H.E. Katz, *J. Appl. Phys.* **81**, 6804 (1997).
2. J.H. Shone, S. Berg. Ch. Kloc, B. Battogg, *Science* **287**, 1022 (2000).
3. S. Radhakrishnan, S.D. Deshpande, *Sensors* **2**, 185 (2002).
4. A. Arshak, S. Zleetni, K. Arshak, *Sensors* **2**, 174 (2002).
5. S. Ambily, C.S. Menon, *Mater. Lett.* **34**, 124 (1998).
6. J.B. Whitlock, P. Panayotatos, G.D. Sharma, M.D. Cox, G.R. Bird, *Opt. Eng.* **32**, 1921 (1993).
7. K.Y. Law, *Chem. Rev.* **93**, 449 (1993).
8. N.B. Mckrown, *Phthalocyanine Materials Synthesis Structured Function* (Oxford: Cambridge University Press: 1998).
9. T. Miyata, S. Kawaguchi, M. Ishi, T. Minami, *Thin Solid Films* **425**, 255 (2003).
10. J. Spadavecchia, G. Ciccarella, G. Vasapollo, P. Siciliano, R. Rella, *Sensor. Actuat. B-Chem.* **100**, 135 (2004).
11. M. Safarikova, I. Safarik, *Eur. Cell. Mater.* **3**, 188 (2002).
12. R. Seoudi, G.S. El-bahy, Z.A. El. Sayed, *Opt. Mater.* **29**, 304 (2006).
13. M. Brinkmann, J.C. Wittmann, C. Chaumont, J.J.Andre, *Thin Solid Films* **292**, 192 (1997).
14. O. Berger, W.J. Fischer, B. Adolphi, S. Tierbach, V. Welev, J.J. Schreiber, *J. Mater. Sci. Electron.* **11**, 331 (2000).
15. L.I. Maissel, R. Glang, *Handbook of Thin Film Technology* (New York: Mc-Graw Hill: 1985).
16. F.H. Moser, A.L. Thomas, *The Phthalocyanines* Vols 1 and 2.
17. J. Bardeen, F.J. Slatt, L.J. Hall, *Photoconductivity Conference,* 146 (New York: Wiley: 1956).
18. A. Susman, *J. Appl. Phys.* **38**, 2738 (1967).
19. M.E. Azim-Araghi, A. Krier, *Pure Appl. Opt.* **6**, 443 (1997).
20. G. Gordillo, J.M. Florez, L.C. Hernandez, *Sol. Energ. Mater. Sol. C.* **37**, 273 (1995).